The investigation of the influence of an applied magnetic field and microwave irradiation on tunnelling luminescence and optically detected magnetic resonance in sodium silicate glasses

1990 J. Phys.: Condens. Matter 2 7453

(http://iopscience.iop.org/0953-8984/2/36/008)

J. Phys.: Condens. Matter 2 (1990) 7453–7464. Printed in the UK

The investigation of the influence of an applied magnetic field and microwave irradiation on tunnelling luminescence and optically detected magnetic resonance in sodium silicate glasses

J M Baker, A A Jenkins, V L Savelev† and W Hayes
Clarendon Laboratory, Parks Road, Oxford OX1 3PU, UK

Received 21 March 1990

Abstract. The influence of magnetic field on tunnelling luminescence in pure sodium silicate glasses has been investigated. It has been shown that the electron (E_1^-) and hole (L^+) centres participating in the tunnelling recombination are paramagnetic. Two types of signal, resonant and non-resonant, were observed upon the application of microwaves (about 24 GHz). The non-resonant signal occurs throughout the whole range of magnetic fields used (up to 4 T) and appears to be due to the hopping migration of the electrons in the conduction band tail. Two resonant signals in the region $g = 2$ were observed and are assigned to recombining electron (E_1^-) and hole (L^+) centres. These signals have a large half-width due to inhomogeneous broadening. The effects of temperature, IR illumination and UV excitation on the magnetic dependence of the intensity of the tunnelling luminescence were studied.

1. Introduction

It is well known that pure sodium silicate glasses exhibit UV luminescence with a maximum at 3.5 eV (Mackey *et al* 1966). This luminescence exists over a wide temperature range (up to 550 K) and may be excited by x-rays (Mackey *et al* 1966) or by UV light from the fundamental absorption region of the glass ($h\nu > 5.5$ eV) (Trukhin *et al* 1980). In addition, the decay of unstable colour centres as a result of thermostimulated processes (Mackey *et al* 1966), or tunnelling recombination (Kangro *et al* 1979), can give rise to this luminescence. The latter is the dominant process at liquid-helium temperature.

It has been shown that the luminescence is intrinsic, and Trukhin *et al* (1980, 1985) have proposed that the structural model for the centre responsible for this luminescence is a quasi-molecular complex $Si–O^-–Na^+$ designated as an L centre.

According to the model for the electron processes which occur in a glass, UV irradiation in the fundamental absorption region causes intracentre excitation of L centres, followed by either intracentre relaxation, resulting in luminescence ($h\nu \simeq 3.5$ eV), or ionisation of the L centres. As a result of the latter, hole (L^+) and electron (E_1^-) centres are formed in the glass. Owing to disorder in the structure of the glass these centres are not mono-energetic but have an energy distribution in the mobility gap.

† Present address: The Institute of Solid State Physics, Latvian State University, 8 Kengaraga iela, 226063, Riga, USSR.

0953-8984/90/367453 + 12 $03.50

Mackey *et al* (1966) established that (E_1^-) centres can be easily bleached by illuminating the glass with light corresponding to their absorption band (1–3 eV), but the hole centres are more stable and cannot be bleached by illuminating in their absorption band.

At temperatures above about 40 K the shallow electron centres are thermally unstable and decay by releasing electrons to the conduction band. Migrating electrons may be trapped followed by recombination resulting in the emission of light quanta (about 3.5 eV). The decay of deeper centres may occur in the same way but requires higher temperatures.

When the temperature is decreased below about 40 K, the release of electrons to the conduction band is suppressed for deeper traps, and less probable for shallow traps. The main mechanism responsible for the luminescence in this case is a tunnelling recombination process (Kangro *et al* 1979). Arbuzov *et al* (1986) found that the tunnelling luminescence intensity in sodium silicate glass was dependent upon temperature between 40 K and 90 K and suggested that the effect was due to electron migration by a hopping mechanism into empty (E_1^-) centres. Earlier this mechanism was suggested for the temperature region 80–160 K by Tale *et al* (1982).

There are a number of papers dedicated to the EPR of sodium silicate glasses (see Griscom (1973–4) and references therein). These experiments were carried out mainly at 239 and 77 K. Some paramagnetic centres were observed, and models have been proposed, but there has been no suggestion that electron (E_1^-) and hole (L^+) centres are responsible for these signals. Usually the EPR experiments were performed separately from luminescence experiments; so it has proved difficult to assign EPR signals to luminescence centres.

Delbecq and Yuster (1975) have found that the application of a magnetic field to crystals leads to quenching of the tunnelling recombination luminescence. Baranov (1982) and Romanov *et al* (1981) applied the technique of optically detected magnetic resonance (ODMR) to investigate tunnelling luminescence in crystals. ODMR allows one to perform EPR and luminescence measurements in the same experiment in order to correlate EPR signals with definite luminescence centres. This method has also been used for the investigation of semiconductors (Nicholls *et al* 1979).

In the present work an attempt was made to study tunnelling luminescence using ODMR.

2. Experimental details

Measurements were made on high-purity glass of composition $Na_2O.3SiO_2$ containing less than 10^{-4} wt% of transition-metal impurities, synthesised from exceptionally pure materials using the technology described by Glebov *et al* (1976).

A sample of typical dimensions 4 mm × 2 mm × 2 mm was placed in a rectangular TE_{102} microwave cavity operating at the K band (about 24 GHz). The cavity was situated in a sample space containing helium exchange gas at a low pressure, which was immersed in a bath of liquid helium. The temperature of the sample space could be reduced to 1.53 K by reducing the pressure above the liquid helium. A carbon resistor, which had been calibrated at the boiling point (4.2 K) and the lambda point (2.17 K) of liquid helium, enabled the temperature to be determined. As the resistor was positioned outside the cavity, the measured temperature was not quite a true reading of the sample temperature.

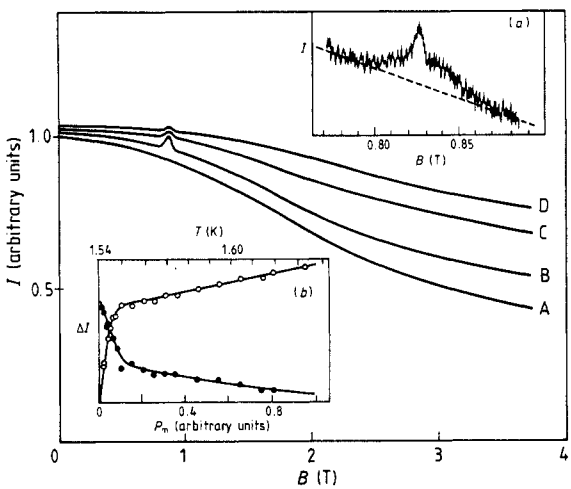

Figure 1. Magnetic field dependence of the luminescence intensity $I(B)$ at different microwave power levels P_m in arbitrary units and temperatures T: curve A, $P_m = 0$, $T = 1.540$ K; curve B, $P_m = 0.15$, $T = 1.555$ K; curve C, $P_m = 0.70$, $T = 1.610$ K; curve D, $P_m = 1.0$, $T = 1.635$ K. Inset (*a*) shows the resonant ODMR signal with the vertical scale magnified 20 times. This also shows the noise level, which has been averaged out in curves A–D. Inset (*b*) shows the microwave power dependence of the resonant (●) and non-resonant (○) signals measured at the same value of B. Also indicated on the top scale of the inset is the temperature measured by the resistance thermometer outside the cavity; this is greater than the temperature of the bath, 1.56 K, because of the microwave heating.

Excitation of the sample was by x-rays or UV light. The x-rays, generated using a Machlett OEG-60 x-ray gun operating at 50 keV and 40 mA, passed through an aluminised Mylar window to irradiate the sample. A deuterium lamp was used as the UV source, access to the sample being gained by a Spectrosil B quartz window. A focal monochromator containing two silica lenses was used to select the UV region (5.5–6.2 eV) of the spectrum. The luminescence passed through a similar quartz window and was focused onto an EMI 9789Q photomultiplier (200–600 nm response).

A 5 T superconducting magnet immersed in the liquid helium was used to investigate the effect of a magnetic field upon this luminescence. The microwaves were generated using an OKI-245 klystron with an output power of 1.2 W at 23.6 GHz. The reflected power (P_m) from the cavity at resonance was monitored on an oscilloscope. Any changes in the total luminescence intensity I, as a result of either microwaves or magnetic field was monitored by the photomultiplier and displayed on a chart recorder. In our results, I is displayed in arbitrary units which are proportional to the output voltage of the photomultiplier.

In our experiments were were interested in the afterglow luminescence. This was produced by irradiating the sample for a specified time (from 15 min to 4 h) after which the source was switched off. It was then necessary to wait for at least 1 h to allow the recombination of the strongly coupled electron–hole pairs, i.e. those whose intercentre distance is small. After this time the rate of decay of luminescence intensity was relatively constant at about 0.6% min^{-1}, and we were then able to investigate the behaviour of the weakly coupled recombining centres. When analysing the results it was necessary to normalise them so as to take into account the continual decay of luminescence for the duration of the measurements.

3. Experimental results

The data in figures 1 and 2 show how various experimental conditions affect the total tunnelling luminescence intensity I as a function of applied magnetic field B, designated

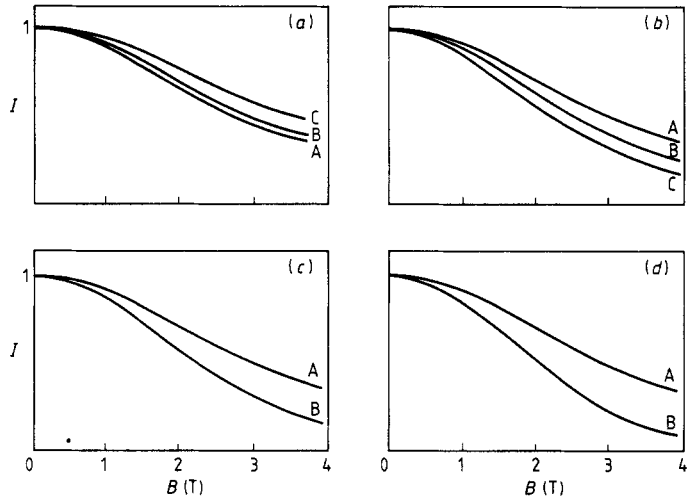

Figure 2. Magnetic field dependence of the luminescence $I(B)$ under different conditions, with zero microwave power. (*a*) Curve A, measured at 1.55 K; curve B, measured at 1.58 K; curve C, measured at 1.91 K. (*b*) Curve A, x-irradiation at 2 K with no further treatment; curve B, after heating (see text); curve C, after IR bleaching (see text). (*c*) Curve A, x-irradiation at 4 K; curve B, x-irradiation at 77 K. (*d*) Curve A, x-irradiation at 4 K; curve B, UV irradiation at 4 K.

as $I(B)$. All data were obtained by chart recording the output of the photomultiplier as the field was swept at 10 mT s^{-1} over the range of measurement. A field sweep from 0 to 4 T and back to 0 T therefore took about 14 min. After such a cycle the reduction in $I(0)$ (about 8%) was the same as it would have been if the field had not been swept, which indicates that the decay of $I(B)$ with time is independent of B. Except for the normalisation for the steady decay of luminescence with time, $I(B)$ was the same for decreasing or increasing B. Such chart recordings are subject to noise. The output has been smoothed out to produce the presented curves, an indication of the noise level being given by inset (*a*) in figure 1.

To obtain the curves shown in figure 1, the sample was x-irradiated at 1.56 K for 2 h and then kept at 1.56 K for 2 h 20 min after the x-rays had been switched off before the measurements of I were started. All of the curves were normalised with respect to curve A at $B = 0$. The conditions of measurement for the curves (given in the figure caption) are the microwave P_m expressed as a decimal fraction of that for maximum output of the klystron (1.2 W) incident on the cavity, and the temperature measured by the resistance thermometer, which shows the temperature rise caused by the application of microwaves, even though the helium bath was maintained at 1.56 K. The microwave power dissipated in the cavity is not well known because it was not possible to match the cavity to the waveguide. The monitoring of reflected power on and off resonance suggests that only 10–20% of the incident power from the klystron was dissipated in the cavity. The dissipation of about 100 mW in the cavity would be expected to maintain the cavity at more than 0.1 K above the temperature of the surrounding helium bath.

Figure 1 shows that the application of microwaves leads to an increase in $I(B)$, and that there are two kinds of change in $I(B)$ or signal: a resonant signal and a non-resonant signal. Inset (*b*) shows the dependence of these signals, and the temperature, upon microwave power.

The resonant signal contains two overlapping lines (inset (*a*) of figure 1): one wide and one relatively narrow. The wide band has a g-value of 1.996 and a half-width Δg of 0.08, and the narrow band has a g-value of 2.005 and a half-width Δg of 0.01. The shape of the resonant signal was the same at all stages of the afterglow.

Figure 2 shows $I(B)$ measured under a variety of conditions without microwaves. All show the same type of decrease with increasing B, but at different rates depending upon the conditions. Curve A in each figure corresponds to approximately the same conditions.

Figure 2(*a*) shows the effect, after x-irradiation at 1.56 K, of changing the temperature at which $I(B)$ was measured, by changing the temperature of the helium bath. Figure 2(*b*) shows the effect of three different treatments between x-irradiation and measurement of $I(B)$ at 1.56 K. For curve A, the treatment was simply to wait for about 2 h. For curve B, the treatment was heating the sample, by admitting a pulse of helium gas at room temperature into the space between the microwave cavity an the helium bath, so that the temperature registered by the thermometer rose to 10 K for a few minutes. For curve C, the treatment was exposure for 10 min to IR irradiation with $h\nu < 1.75$ eV derived from a tungsten lamp with a RG695 filter. Figure 2(*c*) compares the effect of carrying out the x-irradiation at different temperatures before measurement of $I(B)$ at 1.56 K. Figure 2(*d*) compares the effect upon $I(B)$ measured at 1.56 K of x-irradiation and UV irradiation (5.5–6.2 eV), both performed at 4 K; it was checked that the shape of $I(B)$ does not depend upon the duration of the irradiation between 5 min and 2 h and is the same at all stages of afterglow.

4. Discussion

4.1. Magnetic field dependence of the tunnelling luminescence

The fact that the intensity of the tunnelling luminescence $I(B)$ depends upon B (figures 1 and 2) suggests that it is spin dependent, and that the participating electron and hole centres are paramagnetic.

The magnetic field removes the degeneracy of the $\pm\frac{1}{2}$ spin levels, and the energy level scheme for the electron–hole pair, ignoring any interaction, may be represented by figure 3. As recombination can occur only for electron and hole centres with an antiparallel spin orientation, we have allowed for the fact that the rates may be different for spin parallel and antiparallel states; probably R_1 will be greater than R_2 because some spin flip has to occur in the latter process. As our measurements were done on a time scale which allows complete relaxation, we expect a Boltzmann distribution over the four levels: $n_1/n_2 = n_3/n_4 = e^{-x}$ and $n_1/n_3 = n_2/n_4 = e^{-y}$, where $x = g_1\mu_B B/kT$ and $y = g_2\mu_B B/kT$. If we suppose that N is the total number of electron–hole pairs at any time, the solution of the rate equations leads to the following expression for the light energy radiated per unit time:

$$I(B) = \alpha N[R_1(e^{-x} + e^{-y}) + R_2(1 + e^{-x}e^{-y})]/(1 + e^{-x} + e^{-y} + e^{-x}e^{-y}) \tag{1}$$

and hence

$$I(B)/I(0) = \frac{R_1(e^{-x} + e^{-y}) + R_2(1 + e^{-x}e^{-y})}{2(R_1 + R_2)(1 + e^{-x} + e^{-y} + e^{-x}e^{-y})}. \tag{2}$$

In the limit of a high magnetic field,

$$I(B)/I(0) \rightarrow 2/(R_1/R_2 + 1). \tag{3}$$

Then, for example, curve A in figure 1 is well reproduced by taking $R_1/R_2 = 4.1$.

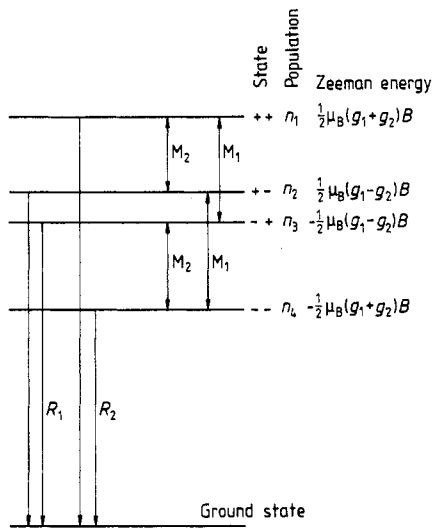

Figure 3. Zeeman splitting of an electron–hole pair. States are labelled with electron and hole spin quantum numbers. M_1 and M_2 are microwave-induced transitions at $h\nu = g_1\mu_B B$ for electrons and $h\nu = g_2\mu_B B$ for holes respectively: The g-values for both types of carrier have been taken to have the same sign. R_1 and R_2 represent radiative recombination rates.

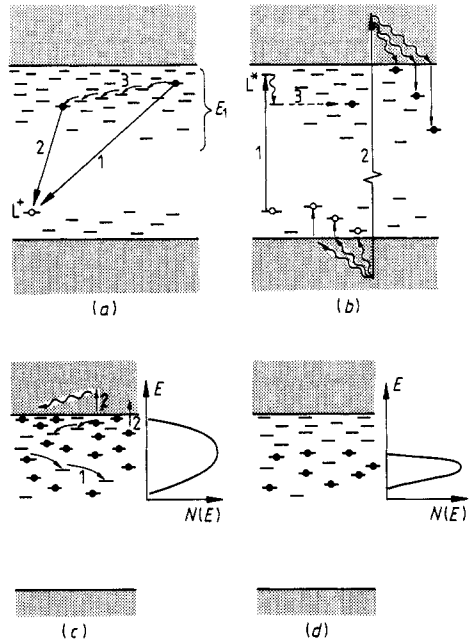

Figure 4. Schematic diagrams of the gap between the conduction and valence bands (both shaded) for some electronic processes in sodium silicate glasses. (*a*) Tunnelling recombination between distant (transition 1) and close (transition 2) electron–hole pairs. Transitions 3 correspond to the hopping migration of electrons. (*b*) Creation of electron and hole centres during UV (transitions 1 and 3) and x-ray (transition 2) irradiation. (*c*) Electron depth distribution $N(E)$ produced after x-irradiation at 4 K, and transitions which subsequently modify $N(E)$: transition 1 is due to hopping migration of electrons produced by heating; transition 2 is due to IR bleaching of E centres. (*d*) Electron depth distribution $N(E)$ produced after x-irradiation at 77 K. A similar concentration of electrons into deeper traps can be created either by starting from $N(E)$ shown in figure 4(*c*) using heating or IR irradiation, or by UV excitation at 4 K.

This suggests that there is not much dependence of the rates R_1 and R_2 upon the value of B.

Some part, but not all, of the differences between the curves in figure 2(*a*) for different temperatures of measurement can be accounted for by different Boltzmann factors, but the remaining differences show that the rates R_1 and R_2 are dependent upon temperature.

All other curves in figure 2 are measured at 1.54 K. They can all be fitted quite well using different values of R_1/R_2; so we need to consider what other factors influence R_1 and R_2 besides the temperature at which $I(B)$ is measured.

These rates will be affected by the rates at which electrons and holes come together to recombine. It is well known that the intensity of tunnelling luminescence depends upon the distance between recombining centres. A previously proposed theoretical model for isolated electron–hole pairs postulates that irradiation creates a characteristic distribution $W(r)$ in the separation r between electron and hole in a pair, and that the probability of recombination is larger for pairs with smaller r (figure 4(*a*)). Hence, if we change $W(r)$ during the decay of afterglow, this will result in changes in luminescence intensity.

Our experiments were performed 1–2 h after irradiation, so that the closest pairs will have recombined. We shall consider two mechanisms which lead to redistribution of trapped electrons; we discuss only the movement of electrons, as hole centres are more stable than electron centres in sodium silicate glasses.

(i) Increasing the sample temperature causes electrons to escape from some traps into the conduction band and to migrate through the sample until they are captured by other traps, thus changing $W(r)$.

(ii) Disorder in amorphous materials leads to a large number of empty localised electron states into which electrons may hop without entering the conduction band (figure 4(*a*)) (Arbuzov *et al* 1986, Tale *et al* 1982); such hopping would occur more frequently as the temperature is raised.

Let us now consider how our experimental data enable us to choose between these two mechanisms.

Figure 2(*c*) shows that $I(B)$ depends upon the temperature at which the irrradiation takes place. This measurement indicates how the temperature dependence of the *filling* of electron traps affects $I(B)$. Sodium silicate glasses have a wide distribution of electron traps with different thermal stabilities. Irradiation of samples at 4 K leads to the filling of both deep and shallow traps, but at 77 K the shallow traps are rapidly emptied by thermally stimulated transitions. Hence, irradiation at 77 K results in the filling of fewer shallow traps than irradiation at 4 K does (figures 4(*c*) and 4(*d*)). The data in figure 2(*c*) suggest that the concentration of electrons into deep traps causes $I(B)$ to decrease more rapidly with increasing B (corresponding to larger R_1/R_2); so the shape of $I(B)$ depends upon the energy depth distribution $N(E)$ of occupied electron levels at the time of measuring $I(B)$; we call $N(E)$ the electron depth distribution.

Our measurements showed that the change in $I(B)$ caused by heating the sample *after* irradiation but *before* measuring $I(B)$ (see, e.g., figure 2(*b*), curves A and B) was observable after x-irradiation at both 4 and 77 K. In order to release trapped electrons after irradiation at 77 K, it would be necessary to raise the temperature of the sample above 77 K. $I(B)$ was always measured in the range 1.53–2 K where there is insufficient thermal energy to release trapped electrons into the conduction band. Hence, the observed thermal effects must be due to the hopping of electrons.

Consider curves A and B in figure 2(*b*). As curve A was measured 2 h after x-irradiation at 2 K, it corresponds to an equilibrium between suppression of afterglow caused by the magnetic field and enhancement of afterglow due to the hopping migration process. Heating the sample to 10 K changes the electron depth distribution in favour of deeper traps, as illustrated in figures 4(*c*) and 4(*d*), which decreases the afterglow (figure 2(*b*), curve B) because hopping migration between deeper states is slower.

IR bleaching of electron centres created by x-irradiation also leads to the emptying of shallow traps through excitation into the conduction band, indicated by the vertical arrows in figure 4(*c*), followed by migration, so changing $N(E)$ from that shown in figure 4(*c*) to that in figure 4(*d*). This accounts for the fact that the observed change in $I(B)$ (curves A–C in figure 2(*b*)) produced by IR irradiation of the sample, after x-irradiation at 2 K, is similar to that produced by heating (curves A and B in figure 2(*b*)).

These data all suggest that the preparation of the sample so that deeper traps are filled before measurement of $I(B)$ at 1.54 K causes R_1/R_2 to increase. The measurement of $I(B)$ at different temperatures shown in figure 2(*a*) also suggests that R_1/R_2 increases with increasing temperature of measurement. This also presumably reflects a concentration of electrons into deeper traps by thermally stimulated hopping migration.

We now consider the results shown in figure 2(*d*). X-ray excitation leads to the creation of electrons and holes owing to band-to-band transitions followed by trapping on electron and hole centres. This leads to a characteristic electron depth distribution in the band tails (figure 4(*b*)). UV excitation leads to creation of electrons and holes by ionisation of L centres. If, after ionisation, the electrons entered the conduction band, we would expect a similar electron depth distribution, and hence $I(B)$, to that for x-rays. The different shape of $I(B)$ for UV excitation shows that a different mechanism must be involved, suggesting that electron traps are not filled through the conduction band.

Trukhin *et al* (1980) established that during UV irradiation (5.5–6.2 eV) of sodium silicate glasses the ionisation of L centres occurs, leading to the creation of L^+ and E_1^- centres. Since curve B for UV excitation in figure 2(*d*) is lower than curve A for x-ray excitation, it can be concluded that ionisation of L centres during UV excitation leads mainly to the population of deep centres. This means that ionisation of L centres occurs not through band states, but by tunnelling, i.e. by transitions from the excited state of the L centre to the localised state of the electron trap, represented by transition 3 in figure 4(*b*).

4.2. Non-resonant signal

As the application of microwaves leads to an increase in sample temperature, at least some of the non-resonant increase in $I(B)$ produced by microwaves is due to their heating effect. As the thermometer is outside the resonant cavity where the heat is generated by the microwaves, it probably records a temperature somewhat lower than that of the sample. In section 3 we suggest that $P_m = 1$ corresponds to about 100 mW of microwave power dissipated in the cavity, which from an approximate calculation of the rate of loss of heat through the exchange gas would suggest a temperature rise of 1–2 K, rather than 0.1 K as measured by the thermometer. This leaves some uncertainty about how much of the non-resonant signal is due to heating, and how much to transition processes induced by the microwaves, such as reorientation of the migrating electron spins during the hopping process, resulting in increased emission. The two distinct parts of the variation in ΔI with P_m (inset (*b*) in figure 1) suggests that the changes are not all due simply to the rise in temperature.

Even at $B = 0$ there is a non-resonant signal which may be due either to a rise in temperature or to microwave-induced transitions during migration. Unfortunately, the change in luminescence with time made it impracticable to measure the effect

upon the absolute level of $I(B)$ of all of the conditions illustrated in figure 2, including change in temperature; the curves are all normalised to $I(0) = 1$. Hence we do not know the magnitude of the effect of a rise in temperature upon $I(0)$. However, during the course of the investigations for curve B in figure 2(*b*), it was noticed that $I(0)$ increased *during* the heating, presumably owing to more rapid tunnelling and recombination.

4.3. The resonant signal

The existence of two resonant signals in $I(B)$ (figures 1(*a*) and 1(*b*)) indicates resonant transitions within recombining paramagnetic centres E_1^- and L^+. Normally, signals with $g < g_e$ (2.0023) correspond to electron centres and those with $g > g_e$ to hole centres; so the measured g-values suggest that the narrow signal at $g = 2.005$ corresponds to the hole centres (L^+) and the broad signal at $g = 1.996$ to electron centres (E_1^-). The lines are much wider than those for similar centres in single-crystal material, which is probably a consequence of inhomogeneous broadening at sites of low symmetry. In conventional EPR of x-irradiated alkali silicate glasses, Bishay (1970) found hole centres in the $g = 2.003$–2.01 region depending upon the composition, and rather wider electron centres near $g = 1.96$.

Trukhin *et al* (1980) suggested a quasi-molecular complex $Si–O^-–Na^+$ as a possible model for the L centre. In this complex, Si–O is mainly covalent, but $O^-–Na^+$ is mainly ionic. This complex could release an electron, so creating a hole centre (L^+), i.e.

$$Si–O^-–Na^+ + h\nu = Si–O^0 \ldots Na^+ + e^-$$

or accept an electron creating an electron centre (L^- or E_1^-), i.e.

$$Si–O^-–Na^+ + e^- = Si–O^- \ldots Na^0.$$

In both cases the ionic bond $O^-–Na^+$ is weakened. However, the oxygen remains strongly coupled with silicon; this link is formed by an oxygen 2p bonding orbital, whereas the ionisation occurs from an oxygen 2p non-bonding orbital. The anisotropy in g-value for oxygen 2p orbitals in both crystalline and glassy SiO_2 (Griscom 1973–4) has been found to vary a great deal depending upon the strength of the crystal field, so that a rather wide line would be expected. If the electron on sodium is in a 3s state, one would not expect its g-value to be much different from the free-spin value, or to be much affected by the known variability between five and six in the number of oxygen ligands of the sodium. However, if the electron were delocalised onto these oxygen ligands, there would be both considerable departure from the free-spin value and considerable width.

Figure 1(*c*) shows the dependence of the resonant and non-resonant signals on microwave power. The power levels were too high to observe the rise in the resonant signal from $P_m = 0$ to a maximum, suggesting that the microwave transitions were heavily saturated. Over the range of P_m for which we have data, the luminescence at resonance rises almost to the value $I(0)$ at the centre of the line from hole centres. For the model proposed in section 4.1 the saturation of either hole or electron resonance would render either e^{-x} or e^{-y} respectively equal to 1. Either of these would make $I(B)/I(0) = 1$. However, the saturation will probably be incomplete in the wider inhomogeneous line from electron centres, so that the signal will be smaller, but the saturation will become nearly complete for the narrow hole centre.

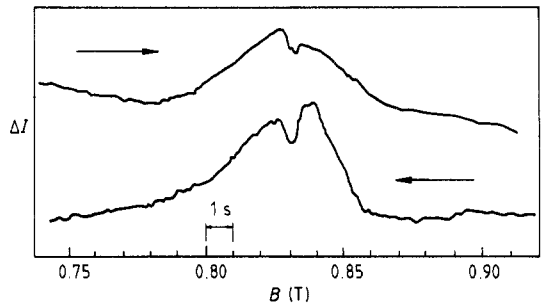

Figure 5. ODMR of the tunnelling luminescence during IR irradiation. The arrows show the direction of sweep of the magnetic field.

IR irradiation of the sample after x-irradiation produces some marked changes in the resonant signal observed both during and after the IR irradiation.

It was seen in section 4.1. that redistribution of electrons released into the conduction band by IR irradiation, and the subsequent filling of traps, produced a more concentrated electron depth distribution which leads to a more rapid decrease in $I(B)$ with increasing B, corresponding to a larger ratio R_1/R_2. It also led to a weakening of the resonant signal, which may simply reflect a decrease in the overall number of electrons and holes, due to recombination stimulated by the IR irradiation.

However, if *during* the IR irradiation, the region of resonant signal is swept through rapidly (about 7 mT s^{-1}), at maximum microwave power, the signal shown in figure 5 is obtained. The signal-to-noise ratio is about 200 times as strong as the normal resonant signal for slow sweep rates (about 5 mT min^{-1}), and it depends upon the direction of sweep. Its magnitude decreased as the sweep rate was decreased. No such phenomenon was observed in a sample which had not been irradiated with IR.

The large signal-to-noise ratio may be explained partially by the much larger luminescence during the IR irradiation process, but the dependence upon sweep rate and direction, and the dip in the region of the hole resonance, suggest that some transient process is involved during the redistribution of electrons excited by the IR irradiation. The rate of population of the states depicted in figure 3 would be expected to be large, and radiative and non-radiative decay may occur before thermalisation. More rapid decay of $+-$ and $-+$ states may leave them depleted relative to $++$ and $--$. As B is increased from below resonance, transient passage through the spin packets on the low-field side of the wide line from electron centres may invert the populations, so transferring a large population from levels 1 and 4 into levels 2 and 3. This would produce a large increase in luminescence. By the time that the field had reached the value for the narrow hole resonance, about half of the electron–hole pairs would have an inverted population distribution. Transitions among these corresponding to the hole resonance should more or less cancel the effect of such transitions among the other half, whose population has not been inverted. Hence the signal in the region of the hole resonance would be mainly due to electron–hole pairs whose g-values are identical; the relaxation conditions for these pairs may lead to a smaller signal, so accounting for the dip at this point. The transitions as that region is traversed would somewhat deplete the populations of levels 1 and 4 of pairs

whose electron centres correspond to spin packets on the high-field side of the wide line, leading to a somewhat smaller signal on that side than on the low-field side.

On sweeping from high to low B the sequence of events would be reversed after the establishment of the transient equilibrium at a high field. Hence it is the high-field side of the electron resonance which would be the stronger. The fact that the whole spectrum is stronger for sweeping from high B may reflect a larger ratio of Boltzmann factors for high B where the energy levels are further apart, and that some partial thermal equilibrium may have been established by spin–lattice relaxation.

5. Conclusions

This first investigation of the optical detection of the effect of microwaves in sodium silicate glasses has shown

(i) that the E_1^- and L^+ centres participating in the tunnelling recombination process are paramagnetic,

(ii) that electron hopping processes play an important role in electronic transport at 4 K,

(iii) that the magnetic field dependence of the luminescence is considerably affected by the energy distribution of electrons in the band states and

(iv) that resonant transitions can be associated with both electron and hole centres.

Acknowledgment

This work was performed as part of the British–Soviet exchange programme, and one of us (VLS) would like to thank the Clarendon Laboratory for the opportunity to experiment on ODMR.

References

Arbuzov V I, Vitolis I K, Kangro A R, Rogulis U T and Tolstoi M M 1986 *Fiz. Khim. Stekla* **12** 75–80

Baranov P G 1982 *Izv. Akad. Nauk SSSR, Ser. Fiz.* **46** 433–9

Bishay A 1970 *J. Non-Cryst. Solids* **3** 54–114

Delbecq C J and Yuster P H 1975 *Phys. Status Solidi* b **68** K21–3

Glebov L B, Popova L B, Tolstoi M N and Rusan V U 1976 *Fiz. Khim. Stekla* **2** 569–71

Griscom D L 1973–4 *J. Non-Cryst. Solids* **13** 251–85

Kangro A R, Tolstoi M N and Vitolis I K 1979 *J. Lumin.* **20** 349–53

Mackey J H, Smith H L and Halperin A 1966 *J. Phys. Chem. Solids* **27** 1759–72

Nicholls J E, Davies J J, Cavenett B C, James J R and Dunstan D J 1979 *J. Phys. C: Solid State Phys.* **12** 361–79

Poole C P Jr 1967 *Electron Spin Resonance. A Comprehensive Treatise on Experimental Techniques* (New York:Wiley)

Romanov N G, Veshchunov Yu P, Vetrov V A and Baranov P G 1981 *Phys. Status Solidi* b **107** K119–24

Tale I A, Zakis Yu R and Gurdziela A S 1982 *Electron Processes and the Structure of Defects in Glass-Systems* pp 94–115 (in Russian)

Trukhin A N, Intenberg L E, Savelev V L, Glebov L B and Tolstoi M N 1985 *Sov. Phys.–Solid State* **27** 1862–4

Trukhin A N, Tolstoi M N, Glebov L B and Savelev V L 1980 *Phys. Status Solidi* b **99** 155–62